Open access • Posted Content • DOI:10.1101/2021.04.06.438731

Functional evaluation of proteolytic activation for the SARS-CoV-2 variant B.1.1.7: role of the P681H mutation — Source link

Bailey Lubinski, Tiffany Tang, Susan Daniel, Javier A. Jaimes ...+1 more authors

Institutions: Cornell University

Published on: 08 Apr 2021 - bioRxiv (Cold Spring Harbor Laboratory)

Topics: Furin

Functional evaluation of proteolytic activation for the SARS-CoV-2 variant B.1.1.7: role of the P681H mutation

Bailey Lubinski [1], Tiffany Tang [2], Susan Daniel [2], Javier A. Jaimes [3 *] and Gary R. Whittaker [3, 4 *]

[1] Graduate Program in Biological & Biomedical Sciences, Cornell University, Ithaca, NY, 14853, USA.

[2] Robert Frederick Smith School of Chemical & Biomolecular Engineering, Cornell University, Ithaca, NY, 14853, USA.

[3] Department of Microbiology & Immunology, College of Veterinary Medicine, Cornell University, Ithaca, NY, 14853, USA.

[3] Master of Public Health Program, Cornell University, Ithaca, NY, 14853, USA.

*Corresponding authors

618 Tower Rd., Ithaca NY 14853, USA

grw7@cornell.edu; jaj246@cornell.edu

Abstract

Severe acute respiratory syndrome coronavirus 2 (SARS-CoV-2) is the agent behind the current COVID-19 pandemic having emerged in Wuhan China in late 2019 from a yet to be determined animal reservoir. SARS-CoV-2 B.1.1.7, a variant identified in the UK in late 2020, contains a higher than typical level of point mutants across its genome, including P681H in the spike S1/S2 cleavage site. Here, we performed assays using fluorogenic peptides mimicking the S1/S2 sequence from Wuhan-Hu1 and B.1.1.7 and observed no definitive difference in furin cleavage between Wuhan-Hu1 and B.1.1.7 *in vitro*. We performed functional assays using pseudo-typed particles harboring SARS-CoV-2 spike proteins and observed no significant differences between Wuhan-Hu1, Wuhan-Hu1 P681H or B.1.1.7 spike-carrying pseudo-typed particles in VeroE6 or Vero-TMPRSS2 cells, despite the spikes containing P681H being more efficiently cleaved. Likewise, we or show no differences in cell-cell fusion assays using the spike P681H-expressing cells. Our findings suggest that while the introduction of P681H in the SARS-CoV-2 B.1.1.7 variant may increase spike cleavage by furin-like proteases, this does not significantly impact viral entry or cell-cell spread. We consider that other factors are at play to account for the increased in transmission and disease severity attributed to this variant of concern (VOC).

Introduction

Severe acute respiratory syndrome coronavirus 2 (SARS-CoV-2) is the agent behind the current COVID-19 pandemic [1]. SARS-CoV-2 emerged from a yet to be determined animal reservoir and was first identified in late 2019; it has since spread rapidly throughout the world. The virus now exists in two lineages, A and B. While both lineages remain in circulation globally, the B lineage became the dominant virus following its introduction into Northern Italy in February 2020. The B lineage has undergone significant diversification as it expanded, and in particular acquired an S gene mutation (D614G) that resulted in a more stabilized spike protein, which has been linked to increased transmissibility [2]. D614G has now become established in circulating B lineage viruses.

In late summer to early fall 2019, a new variant of SARS-CoV-2 was identified in the UK, based on S-gene target failures in community-based diagnostic PCR testing [3]. Following subsequent sequence analysis, this variant was defined as variant of concern (VOC) B.1.1.7/501Y.V1 by Public Health England. B.1.1.7 rapidly expanded across the south of England and subsequently spread to other parts of the U.K. [4], and now globally. The B.1.1.7 VOC was unusual compared to other SARS-CoV-2 variants emerging at that time in that is contained a higher than typical level of point mutants across its genome; 23 in total. Of particular note were nine mutations in the spike gene compared to prototype sequences; a 69-70 deletion (the cause of S-gene target failure), Y144 del, N501Y, A570D, D614G, P681H, T716I, S982A, and D118H, with seven of these distinct to B.1.1.7. One of the more concerning mutations was N501Y, which was linked (along with D614G) to increased affinity of the spike protein to the SARS-CoV-2 receptor (ACE-2). N501Y has subsequently been found in other VOCs circulating around the world, i.e., B.1.351 and B.1.1.28.1 (P.1) [5-7]

Since its first identification, SARS-CoV-2 B.1.1.7 has undergone extensive characterization. Current consensus indicates that this VOC has a transmission advantage in the community [4,8], possibly

accompanied by increased disease severity [9], but it does not appear evade immune surveillance by natural immunity or vaccination. One hypothesis is that that the B.1.1.7 variant acquired its extensive range of mutations in a single immunocompromised individual [3] who then initiated a super-spreader event that gave rise to the subsequent dissemination of the lineage, as previously proposed for influenza virus [10].

The P681H mutation of B.1.1.7 is of note as it is part of a proteolytic cleavage site for furin and furin-like proteases at the junction of the spike protein receptor-binding (S1) and fusion (S2) domains [11]. The S1/S2 junction of the SARS-CoV-2 S gene has a distinct indel compared to all other SARS-like viruses (sarbecoviruses in betacoronavirus lineage B)—the amino acid sequence of SARS-CoV-2 S protein is $_{681}$-P-R-R-A-R|S-$_{686}$ with proteolytic cleavage (|) predicted to occur between the arginine and serine residues depicted. Based on nomenclature established for proteolytic events [12], the R|S residues are defined as the P1|P1' residues for enzymatic cleavage, with 681H of B.1.1.7 S being the P5 cleavage position. The ubiquitously-expressed serine protease furin is highly specific and cleaves at a distinct multi-basic motif containing paired arginine residues; furin requires a minimal motif of R-x-x-R (P4-x-x-P1), with a preference for an additional basic residue at P2; i.e., R-x-B-R [13]. For SARS-CoV-2, the presence of the S1/S2 "furin site" enhances virus transmissibility [14,15]. For B.1.1.7 S, P681H (P5) may provide an additional basic residue (especially at low pH) and modulate S1/S2 cleavability by furin, and hence virus infection properties.

We previously studied the role of proteolytic activation of the spike protein of the prototype lineage B SARS-CoV-2 (isolate Wuhan-Hu1). Here, we used a similar approach to study the role of the proteolytic activation of the spike protein in the context of the B.1.1.7 VOC, with a focus on the P681H point mutant.

Methods

Furin prediction calculations. Prop: CoV sequences were analyzed using the ProP 1.0 Server hosted at: cbs.dtu.dk/services/ProP/. PiTou: CoV sequences were analyzed using the PiTou V3 software hosted at: http://www.nuolan.net/reference.html.

Fluorogenic peptide assays

Fluorogenic peptide assays were performed as described previously with minor modifications [16]. Each reaction was performed in a 100 μL volume consisting of buffer, protease, and SARS-CoV-2 S1/S2 WT (TNSPRRARSVA) or SARS-CoV-2 S1/S2 B.1.1.7 (TNSHRRARSVA) fluorogenic peptide in an opaque 96-well plate. For trypsin catalyzed reactions, 0.8 nM/well TPCK trypsin was diluted in PBS buffer. For furin catalyzed reactions, 1 U/well recombinant furin was diluted in buffer consisting of 20 mM HEPES, 0.2 mM CaCl2, and 0.2 mM β-mercaptoethanol, at pH 6.5, 7.0 or 7.5. Fluorescence emission was measured once per minute for 60 continued minutes using a SpectraMax fluorometer (Molecular Devices) at 30 °C with an excitation wavelength of 330 nm and an emission wavelength of 390 nm. Vmax was calculated by fitting the linear rise in fluorescence to the equation of a line.

Synthesis and Cloning of the B.1.1.7 spike protein. The B.1.1.7 spike gene from isolate hCoV-19/England/MILK-9E05B3/2020 (EPI_ISL_601443) was codon-optimized, synthesized and cloned into a pcDNA 3.1+ vector for expression (GenScript).

Site-directed Mutagenesis

Mutagenesis primers (cagacctggctctcctgtgggagtttgtctgggt/ acccagacaaactcccacaggagagccaggtctg) were designed based on the DNA sequence for SARS-CoV-2 Wuhan-Hu1 using the Agilent QuickChange Primer Design tool. Mutagenesis was carried out on a pCDNA-SARs2 Wuhan-Hu 1 S plasmid to create the P681H mutation, using the Agilent QuickChange Lightning Mutagenesis kit (The original

plasmid was generously provided by David Veesler, University of Washington USA). XL-10 gold competent cells were transformed with the mutated plasmid, plated on LB Agar + Ampicillin plates, and left at 37°C overnight. A distinct colony was chosen the next day to grow up a 4 ml small culture at 37°C overnight. pCDNA-SARC-CoV-2 Wuhan-Hu1 P681H S plasmid was then extracted using the Qiagen QIAprep Spin Miniprep Kit and Sanger Sequencing was used to confirm incorporation of the mutation.

Pseudoparticle Generation

HEK293T cells were seeded at 3x10e5 cells/ml in a 6 well plate the day before transfection. Transfection was performed using polyethylenimine (PEI) and 1X Opti-Mem from Gibco. Cells were transfected with 800ng of pCMV-MLV-gagpol, 600ng of pTG-luc, and 600 ng of a plasmid containing the viral envelope protein of choice. Viral envelope plasmids included pCAGGS-VSV G as a positive control, pCDNA-SARS-CoV-2 Wuhan-Hu1 S, pCDNA- SARS-CoV-2 Wuhan-Hu1 P681H S, and pCDNA- SARS-CoV-2 B.1.1.1.7 S. pCAGGS was used for a Δ-Envelope negative control. 48 hours post transfection, supernatant containing the pseudoparticles was removed, centrifuged to remove cells debris, filtered, and stored at -80°C.

Pseudoparticle Infection Assay

Vero E6 and Vero TMPRSS2 cells were seeded at 3e5 cells/ml in a 24 well plate the day before infection. Cells were washed three times with 1X DPBS and then infected with 700 ul of either VSV G, SARS-CoV-2 S, SARS-Cov-2 P681H S, SARS-CoV-2 B.1.1.1.7 S, or Δ-Envelope pseudoparticles. Infected cells incubated on a rocker for 1.5 hours at 37°C, and then 300 ul of complete media was added and cells were left at 37°C. At 72 hours post-infection, cells were lysed and the level of infection was assessed using the Promega Luciferase Assay System. The manufacturer's protocol was modified by putting the cells through 3 freeze/thaw cycles after the addition of 100 ul of the lysis reagent. 10 ul

of the cell lysate was added to 20 ul of luciferin, and then luciferase activity was measured using the Glomax 20/20 luminometer (Promega). Infection assays were done in triplicate and were replicated 4 times. All four replicates were carried out using pseudoparticles generated from the same transfection.

Western blot analysis of pseudoparticles.

3 mL of pseudoparticles were pelleted using a TLA-55 rotor with an Optima-MAX-E ultracentrifuge (Beckman Coulter) for 2 hours at 42,000 rpm at 4°C. Particles were resuspended in 30 μL DPBS buffer. Sodium dodecyl sulfate (SDS) loading buffer and DTT were added to samples and heated at 65°C for 20 minutes. Samples were separated on NuPAGE Bis-Tris gel (Invitrogen) and transferred on polyvinylidene difluoride (PVDF) membranes (GE). SARS-CoV-2 S was detected using a rabbit polyclonal antibody against the S2 domain (Cat: 40590-T62, Sinobiological) and an AlexaFluor 488 goat anti-rabbit antibody. Bands were detected using the ChemiDoc Imaging software (Bio-Rad) and band intensity was calculated using the analysis tools on Biorad Image Lab 6.1 software to determine the uncleaved to cleaved S ratios.

Cell-Cell Fusion Assay

VeroE6 and Vero-TMPRSS2 cells were transfected with a plasmid harboring the spike gene of the SARS-CoV-2 isolate Wuhan-Hu 1, SARS-CoV-2 B.1.1.7 variant, the SARS-CoV-2 isolate Wuhan-Hu 1 with a P681H mutation, or a delta-spike pCDNA3.1+ plasmid, and evaluated through an immunofluorescence assay (IFA). Transfection was performed 8-well glass slides at a 90% confluent cells using Lipofectamine® 3000 (Cat: L3000075, Invitrogen Co.), following the manufacturer's instructions and a total of 250 ng of DNA per well was transfected. The cells were then incubated at 37 ˚C with 5% of CO2 for 28 hours. For the IFA, cells were fixed with 4% paraformaldehyde for 15 minutes and quenched with 50 mM NH_4Cl. Permeabilization was performed with 0.1% Triton X-100 in PBS for 5 minutes on ice. Blocking was performed using 5% heat inactivated goat serum in PBS

for 20 minutes and the antibodies for labeling were diluted in the same solution. The spike expression was detected using the SARS-CoV-2 spike antibody (Cat: 40591-T62, Sino Biological Inc.) at 1/500 dilution for 1 hour. Secondary antibody labeling was performed using AlexaFluorTM 488 goat anti-rabitt IgG antibody (Cat: A32731, Invitrogen Co.) at a 1/500 dilution for 45 minutes. Three washes with PBS were performed between each step of the assay. Finally, slides were mounted using DAPI Fluoromount-G® (Cat: 0100-20, SouthernBiotech Inc.) and analyzed with fluorescent.

Results

Bioinformatic and biochemical analysis of the SARS-CoV-2 B.1.1.7 S1/S2 cleavage site

To gain insight into proteolytic processing at the S1/S2 site of the B.1.1.7 spike protein, we first took a bioinformatic approach utilizing the PiTou [17] and ProP [18] cleavage prediction tools, comparing B.1.1.7 to the prototype virus Wuhan-Hu1—as well as to SARS-CoV-1, MERS-CoV, and selected other human respiratory betacoronaviruses (HCoV-HKU1 and HCoV-OC43); Figure 1. Both algorithms predicted a small increase in the furin cleavage for B.1.1.7 compared to Wuhan-Hu1; in comparison SARS-CoV-1 is not predicted to be furin-cleaved; as expected, MERS-CoV showed a relatively low furin cleavage score with HCoV-HKU1 and HCoV-OC43 showing much higher furin cleavage scores.

Virus	S1/S2 Sequence	Furin Score PiTou	Furin Score ProP
SARS-CoV-2	672-ASYQTQTNSP**RR**A**R**|SVASQS-691	+ 9.196	0.620
SARS-CoV-2 (B117)	669-ASYQTQTNS**H**RRA**R**|SVASQS-688	+ 9.907	0.704
SARS-CoV-1	654-AGICASYHTVSLL**R**|STSQ**K**S-673	– 5.167	0.123
MERS-CoV	738-LPDTPSTLTP**R**SV**R**|SVPGEM-757	+ 5.155	0.563
HCoV-HKU1	747-YNSPSSSSS**RRKRR**|SISASY-766	+ 14.634	0.918
HCoV-OC43 (clinical)	750-GYCVDYFKN**RR**S**RR**|AITTGY-769	+ 10.10	0.736

Figure 1. Furin cleavage score analysis of CoV S1/S2 cleavage sites. CoV S sequences were analyzed using the ProP 1.0 and PiTou 3.0 furin prediction algorithm, generating a score with bold numbers indicating predicted furin cleavage. (\|) denotes the position of the predicted S1/S2 cleavage site. Basic resides, arginine (R) and lysine (K), are highlighted in blue, with histidine (H) in purple. Sequences corresponding to the S1/S2 region of SARS-CoV-2 (QHD43416.1), SARS-CoV (AAT74874.1), MERS-CoV (AFS88936.1), HCoV-HKU1 (AAT98580.1), HCoV-OC43 (KY369907.1) were obtained from GenBank. Sequences corresponding to the S1/S2 region of SARS-CoV-2 B.1.1.7 (EPI_ISL_1374509) was obtained from GISAID.

To directly address the activity of furin on the SARS-CoV-2 B.1.1.7 S1/S2 site, we used a biochemical peptide cleavage assay [16]. The specific peptide sequences used here were TNSPHRRARSVA (B.1.1.7 S1/S2). TNSPRRARSVA (Wuhan-Hu1 S1/S2). We tested furin, along with trypsin as a control. We also assessed the effect of lowered pH because of the known properties of histidine (H) to have an ionizable side chain with a p*Ka* near neutrality [19] (Figure 2). As predicted, furin effectively cleaved Wuhan-Hu1 (WT) S1/S2, with B.1.1.7 S1/S2 showing a slight increase in cleavage at pH 7.5. At pH 7.0 and pH6.5, B.1.1.7 S1/S2 was actually less efficiently cleaved than WT, with cleavage not measurable below pH 6.5. Trypsin cleaved both peptides, but was less efficient than furin (at pH 7.4). This comparative data with SARS-CoV S1/S2 sites reveals that the acquisition of the 618H mutation does not significantly increase cleavability by furin, and may in fact be inhibitory.

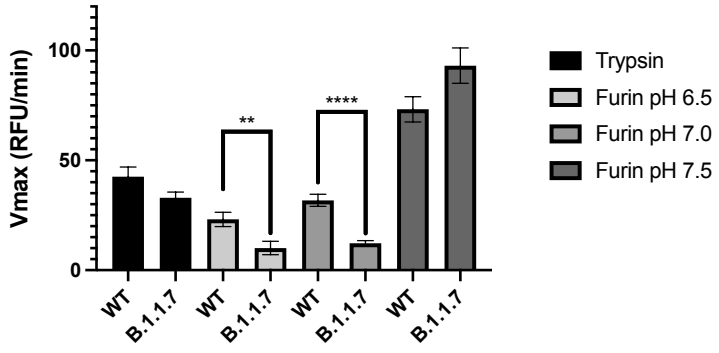

Figure 2. Fluorogenic peptide cleavage assays of the SARS-CoV-2 S1/S2 cleavage site. Peptides mimicking the S1/S2 site of the SARS-CoV-2 WT and B.1.1.7 variants were evaluated for *in vitro* cleavage by trypsin and furin proteases at pH 7.4 (trypsin), and pH 6.5, 6.0 and 7.5 (furin) conditions. A significant decrease in the cleavage of the B.1.1.7 S1/S2 peptide by furin was observed at pH 6.5 and 7.0 compared to WT. In contrast, a non-significant increase in the furin cleavage of the B.1.1.7 peptide was observed at pH 7.5.

Functional analysis of virus entry using viral pseudoparticles

To assess the functional importance of the S1/S2 site for SARS-CoV-2 entry, we utilized pseudoparticles consisting of a murine leukemia virus (MLV) core displaying a heterologous viral envelope protein to recapitulate the entry process of the native counterpart—particles also contain a luciferase reporter that integrates into the host cell genome to drive expression of luciferase, which is quantifiable [20]. In this study, MLV pseudoparticles containing the B.1.1.7, Wuhan-Hu1 SARS-CoV-2 S protein (WT), and a P681H point mutant of Wuhan-Hu1 were also generated alongside positive

control particles containing the vesicular stomatitis virus (VSV) G protein, along with negative control particles (Δenvpp) lacking envelope proteins (not shown), using the HEK293T cell line for particle production.

We examined infection of SARS-CoV-2 pseudo-particles in cell lines representative of both the "early" and "late" cell entry pathways (Figure 3), as the entry mechanisms of SARS-CoV-2 can be highly cell-type dependent [1]. In this study, we utilized the Vero-TMPRSS2 ("early pathway") and the Vero-E6 ("late pathway") cell lines, which are predicted to activate the SARS-CoV-2 S2' using TMPRSS2 and cathepsin L respectively. While Vero-TMPRSS2 cells gave overall higher luciferase signal indicative of more efficient entry, we observed little difference in infection between pseudoparticles displaying spike protein from either B.1.1.7, Wuhan-Hu1 (WT) or Wuhan-Hu1 P681H. As expected, VSVpp (positive control) infected both cell lines with several orders of magnitude higher luciferase units than the values reported with Δenvpp infection (negative control).

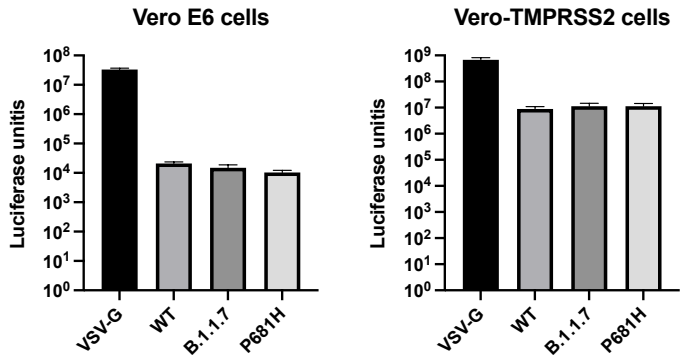

Figure 3. Pseudoparticle infectivity assays in VeroE6 and Vero-TMPRSS2 cells. VeroE6 and Vero-TMPRSS2 cells were infected with MLVpps harboring the VSV-G, SARS-CoV-2 S WT, SARS-CoV-2 S B.1.1.7 variant, SARS-CoV-2 S WT with P681H mutation. Data represents the average luciferase activity of cells of three biological replicates. No significant differences in luciferase transduction were observed between the infected cells.

The pseudoparticles were also probed for their S content via western blot and densitometry. For both B.1.1.7 and Wuhan-Hu1 P681H particles, we detected increased cleavage of the spike protein compared to Wuhan-Hu1 (WT); see Table 1. In light of the peptide cleavage data from Figure 2, it is unclear if this increased cleavage is mediated by furin or another cellular protease, possibly another

member of the proprotein convertase (PC) family, of which furin is a member (furin is also defined as *PCSK3*/PC3) [21].

Spike protein	Ratio cleaved S : uncleaved S
Wuhan-Hu1 (WT)	4.5 : 1
B.1.1.7	22 : 1
Wuhan-Hu1 (P681H)	14 :1

Table 1. Ratio of the intensity of cleaved S band to uncleaved S in MLV pseudoparticles. Western blot analysis of MLV pseudoparticles carrying the WT, B.1.1.7, or P681H S was conducted using an antibody targeting the SARS-CoV-2 S2 domain (Sino Biological). Band intensity was normalized to the uncleaved band intensity of each pseudoparticle.

Functional analysis of membrane fusion activity

To explore more directly the fusion capability of the B.1.1.7 spike protein, we performed a cell-to-cell fusion assay (Figure 4). Vero-TMPRSS2 and VeroE6 cells were transfected with the B.1.1.7, Wuhan-Hu1 (WT) and Wuhan-Hu1 P681H spike gene and we then evaluated syncytia formation as a read-out of membrane fusion. While Vero-TMPRSS2 cells formed more extensive syncytia than VeroE6 cells, we observed no difference in the syncytia formation following spike protein expression for either B.1.1.7, Wuhan-Hu1 (WT) or Wuhan-Hu1 P681H. These data show that the P681H mutation had no effect on membrane fusion activity of the SARS-CoV-2 spike protein under the conditions tested.

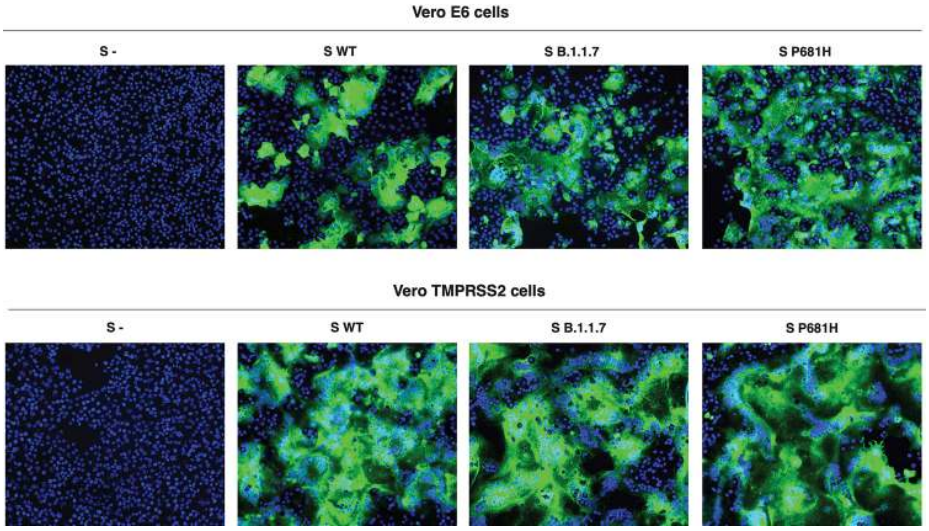

Figure 4. Cell-cell assays of S-expressing VeroE6 and Vero-TMPRSS2 cells. Cells were transfected with the SARS-CoV-2 WT, B.1.1.7 or P681H S gene and syncytia formation was evaluated through IFA after 28 hours. Syncytia was observed in all cells, regardless the expressed S type. More extensive syncytia formation was observed in Vero-TMPRSS2 cells and was consistent among the three S proteins.

Discussion

Here, we performed *in vitro* assays using fluorogenic peptides mimicking the S1/S2 sequence from both Wuhan-Hu1 and B.1.1.7 and observed no definitive difference in furin cleavage for B.1.1.7. We performed functional assays using pseudo-typed particles harboring SARS-CoV-2 spike proteins and observed no significant transduction differences between Wuhan-Hu1 and B.1.1.7 spike-carrying pseudo-typed particles in VeroE6 or Vero-TMPRSS2 cells, despite the spikes containing P681H being more efficiently cleaved. Likewise, we or show no differences in cell-cell fusion assays using the spike P681H-expressing cells. Our findings suggest that the introduction of P681H in the B.1.1.7 variant may increase spike cleavage by furin-like proteases, but this does not significantly impact viral entry or cell-cell spread. We consider that other factors are at play to account for the increased in transmission and disease severity attributed to the SARS-CoV-2 B.1.1.7 VOC.

Overall, we show that the P681H mutation at the S1/S2 site of the SARS-CoV-2 spike protein may increase its cleavability by furin-like proteases, but that this does not translate into increased virus entry or membrane fusion. These findings are broadly in line with those of Brown *et al.* [22] using infectious SARS-CoV-2, who showed no differences in the B.1.1.7 variant in terms of viral replication in primary human airway cells—but did show a disadvantage in Vero cells linked to increased cleavage of the spike protein. In contrast, Dicken *et al.* [23] indicated enhanced entry of B.1.1.7, but in this case only under conditions with low expression of the ACE-2 receptor.

B.1.1.7 is certainly not the only SARS-CoV-2 variant with a P681H change in the spike protein; it is also present in B.1.243 (clade 20A), B.1.222 (clade 20B) and a lineage B.1 variant termed clade 20C, with these three variants recently reported in New York State, USA [24]. Interestingly, B.1.243 comprised the majority of P681H-containing viruses and was the predominant variant in New York in November 2020, but had declined significantly by February 2021 (to be replaced by B.1.1.7 and B.1.222 among

other variants)—some of which do not contain P681H (e.g., B.1.429). Other examples of variants of interest (VOIs) containing P681H include A.VOI.V2 detected through travel surveillance in Angola, Africa [25], isolates from Hawaii [26] and viruses originally classified under lineage B.1.1.28 in locations such as the Philippines [27]. However, many other VOIs e.g., CAL.20C [28] do not contain P681H. Other variants containing mutations have been identified that have been proposed to impact S1/S2 cleavage, e.g., A688V [29], but we consider such mutations to be too distal to the cleavage site to have a direct impact on furin activity.

The SARS-CoV-2 S1/S2 site contains three basic residues in atypical spacing for a furin cleavage site [30], and as such is not "polybasic". The P681H mutation increases the number of basic residues to four (especially at lowered pH) and is predicted to result in a slightly increased cleavability based on ProP and Pitou scoring and peptide cleavage assays at pH 7.4 (Fig. 1). However, it is important to note that the P681H change does not result in the formation of a consensus furin cleavage site (i.e., ^{P4}R-x-B-R^{P1}), even at lowered pH. It is also of note that increased spike protein cleavage does not always translate into increased function and may in fact be detrimental. A good example of this is the insertion of furin cleavage sites into SARS-CoV-1 spike at S1/S2 and/or S2', which resulted in a hyper-fusogenic phenotype [31,32], but with pseudoparticles being unrecoverable especially when added at S2'—presumably due to the presence of an unstable spike protein. One interpretation of the appearance of the P681H mutation in circulating viruses is that SARS-CoV-2 is evolving to become a transmissible but relatively benign community-acquired respiratory (CAR) or "common cold" coronavirus [33], such as the betacoronaviruses HCoV-HKU1 and HCoV-OC43—both of which have very strong "polybasic" furin cleavage sites at the S1/S2 position (Fig. 1). It remains to be determined how any increased cleavage of SARS-CoV-2 S may affect factors such as increased duration of viral shedding, which is one possible explanation of increased transmissibility for B.1.1.7. [34].

As explained for other variants (including D614G in humans and Y453F in mink [6]), we consider that the rise of P681H-containing viruses could be due to chance, with founder effects being responsible for rapid progression, or P681H may confer an advantage with regards transmissibility or cell-cell spread *in vivo*. Our data here reinforce the concept that while analysis of individual point mutations is critical part of understanding virus biology, a full assessment of the epidemiological context of virus infection requires more extensive study [35]. It will continue to be important to track VOCs and VOIs. While the VOCs B.1.351 and B.1.1.28.1 (P.1) are currently of high concern due to immune escape [7,36-39], B.1.1.7 is not presently a concern in this regard [40]; however, the possible acquisition of "immune-escape" mutations such as E484K or N439K [41,42] during widespread circulation in the population means that SARS-CoV-2 B.1.1.7 remains a significant concern.

Acknowledgements

This work was funded by the National Institute of Health research grant R01AI35270. TT is supported by the National Science Foundation Graduate Research Fellowship Program under Grant No. DGE-1650441 and the Samuel C. Fleming Family Graduate Fellowship. We would especially like to thank Jean Millet, Hector Aguilar-Carreno and Ruth Collins for important insight, and all members of the Daniel and Whittaker groups for helpful discussions.

References

1 Whittaker, G. R., Daniel, S. & Millet, J. K. Coronavirus entry: how we arrived at SARS-CoV-2. *Curr Opin Virol* **47**, 113-120, doi:10.1016/j.coviro.2021.02.006 (2021).

2 Zhou, B. *et al.* SARS-CoV-2 spike D614G change enhances replication and transmission. *Nature* **592**, 122-127, doi:10.1038/s41586-021-03361-1 (2021).

3 Rambaut, A. *et al.* Preliminary genomic characterisation of an emergent SARS-CoV-2 lineage in the UK defined by a novel set of spike mutations, <https://virological.org/t/preliminary-genomic-characterisation-of-an-emergent-sars-cov-2-lineage-in-the-uk-defined-by-a-novel-set-of-spike-mutations/563> (2021).

4 Volz, E. *et al.* Assessing transmissibility of SARS-CoV-2 lineage B.1.1.7 in England. *Nature*, doi:10.1038/s41586-021-03470-x (2021).

5 Tegally, H. *et al.* Detection of a SARS-CoV-2 variant of concern in South Africa. *Nature*, doi:10.1038/s41586-021-03402-9 (2021).

6 Lauring, A. S. & Hodcroft, E. B. Genetic Variants of SARS-CoV-2-What Do They Mean? *JAMA* **325**, 529-531, doi:10.1001/jama.2020.27124 (2021).

7 Coutinho, R. M. *et al.* Model-based estimation of transmissibility and reinfection of SARS-CoV-2 P.1 variant. *medRxiv*, 2021.2003.2003.21252706, doi:10.1101/2021.03.03.21252706 (2021).

8 Davies, N. G. *et al.* Estimated transmissibility and impact of SARS-CoV-2 lineage B.1.1.7 in England. *Science*, eabg3055, doi:10.1126/science.abg3055 (2021).

9 Challen, R. *et al.* Risk of mortality in patients infected with SARS-CoV-2 variant of concern 202012/1: matched cohort study. *BMJ* **372**, n579, doi:10.1136/bmj.n579 (2021).

10 Xue, K. S. *et al.* Parallel evolution of influenza across multiple spatiotemporal scales. *Elife* **6**, doi:10.7554/eLife.26875 (2017).

11 Jaimes, J. A., Andre, N. M., Chappie, J. S., Millet, J. K. & Whittaker, G. R. Phylogenetic Analysis and Structural Modeling of SARS-CoV-2 Spike Protein Reveals an Evolutionary Distinct and Proteolytically Sensitive Activation Loop. *J Mol Biol* **432**, 3309-3325, doi:10.1016/j.jmb.2020.04.009 (2020).

12 Polgár, L. in *Mechanisms of Protease Action* Ch. 2, 43-86 (CRC press, 1989).

13 Seidah, N. G. & Prat, A. The biology and therapeutic targeting of the proprotein convertases. *Nat Rev Drug Discov* **11**, 367-383, doi:10.1038/nrd3699 (2012).

14 Johnson, B. A. *et al.* Loss of furin cleavage site attenuates SARS-CoV-2 pathogenesis. *Nature* **591**, 293-299, doi:10.1038/s41586-021-03237-4 (2021).

15 Peacock, T. P. *et al.* The furin cleavage site of SARS-CoV-2 spike protein is a key determinant for transmission due to enhanced replication in airway cells. *bioRxiv*, 2020.2009.2030.318311, doi:10.1101/2020.09.30.318311 (2020).

16 Jaimes, J. A., Millet, J. K. & Whittaker, G. R. Proteolytic Cleavage of the SARS-CoV-2 Spike Protein and the Role of the Novel S1/S2 Site. *iScience* **23**, 101212, doi:10.1016/j.isci.2020.101212 (2020).

17 Tian, S., Huajun, W. & Wu, J. Computational prediction of furin cleavage sites by a hybrid method and understanding mechanism underlying diseases. *Sci Rep* **2**, 261, doi:10.1038/srep00261 (2012).

18 Duckert, P., Brunak, S. & Blom, N. Prediction of proprotein convertase cleavage sites. *Protein Eng Des Sel* **17**, 107-112, doi:10.1093/protein/gzh013 (2004).

19 Nelson, D. L. & Cox, M. M. *Lehninger Principles of Biochemistry*. (Worth Publishers, 2000).

20 Millet, J. K. *et al.* Production of Pseudotyped Particles to Study Highly Pathogenic Coronaviruses in a Biosafety Level 2 Setting. *J Vis Exp*, doi:10.3791/59010 (2019).

21 Garten, W. Characterization of Proprotein Convertases and Their Involvement in Virus Propagation, in *Activation of Viruses by Host Proteases* (ed E. Böttcher-Friebertshäuser *et al.*) 205-248 (Springer Nature, 2018).

22 Brown, J. C. *et al.* Increased transmission of SARS-CoV-2 lineage B.1.1.7 (VOC 2020212/01) is not accounted for by a replicative advantage in primary airway cells or antibody escape. *bioRxiv*, 2021.2002.2024.432576, doi:10.1101/2021.02.24.432576 (2021).

23 Dicken, S. J. *et al.* Characterisation of B.1.1.7 and Pangolin coronavirus spike provides insights on the evolutionary trajectory of SARS-CoV-2. *bioRxiv*, doi:10.1101/2021.03.22.436468 (2021).

24 Lasek-Nesselquist, E., Pata, J., Schneider, E. & George, K. S. A tale of three SARS-CoV-2 variants with independently acquired P681H mutations in New York State. *medRxiv*, 2021.2003.2010.21253285, doi:10.1101/2021.03.10.21253285 (2021).

25 De Oliveira, T. & et.al. A novel variant of interest of SARS-CoV-2 with multiple spike mutations detected through travel surveillance in Africa, <https://www.krisp.org.za/publications.php?pubid=330> (2021).

26 Maison, D. P., Ching, L. L., Shikuma, C. M. & Nerurkar, V. R. Genetic Characteristics and Phylogeny of 969-bp S Gene Sequence of SARS-CoV-2 from Hawaii Reveals the Worldwide Emerging P681H Mutation. *bioRxiv*, 2021.2001.2006.425497, doi:10.1101/2021.01.06.425497 (2021).

27 Tablizo, F. A. *et al.* Genome sequencing and analysis of an emergent SARS-CoV-2 variant characterized by multiple spike protein mutations detected from the Central Visayas Region of the Philippines. *medRxiv*, 2021.2003.2003.21252812, doi:10.1101/2021.03.03.21252812 (2021).

28 Zhang, W. *et al.* Emergence of a Novel SARS-CoV-2 Variant in Southern California. *JAMA*, doi:10.1001/jama.2021.1612 (2021).

29 Tegally, H. *et al.* Sixteen novel lineages of SARS-CoV-2 in South Africa. *Nat Med* **27**, 440-446, doi:10.1038/s41591-021-01255-3 (2021).

30 Tang, T. *et al.* Proteolytic Activation of SARS-CoV-2 Spike at the S1/S2 Boundary: Potential Role of Proteases beyond Furin. *ACS Infect Dis* **7**, 264-272, doi:10.1021/acsinfecdis.0c00701 (2021).

31 Belouzard, S., Chu, V. C. & Whittaker, G. R. Activation of the SARS coronavirus spike protein via sequential proteolytic cleavage at two distinct sites. *Proc Natl Acad Sci U S A* **106**, 5871-5876, doi:10.1073/pnas.0809524106 (2009).

32 Follis, K. E., York, J. & Nunberg, J. H. Furin cleavage of the SARS coronavirus spike glycoprotein enhances cell-cell fusion but does not affect virion entry. *Virology* **350**, 358-369, doi:10.1016/j.virol.2006.02.003 (2006).

33 Jin, X. *et al.* Virus strain from a mild COVID-19 patient in Hangzhou represents a new trend in SARS-CoV-2 evolution potentially related to Furin cleavage site. *Emerg Microbes Infect* **9**, 1474-1488, doi:10.1080/22221751.2020.1781551 (2020).

34 Kissler, S. M. *et al.* Densely sampled viral trajectories suggest longer duration of acute infection with B.1.1.7 variant relative to non-B.1.1.7 SARS-CoV-2. *medRxiv*, 2021.2002.2016.21251535, doi:10.1101/2021.02.16.21251535 (2021).

35 Goodman, L. B. & Whittaker, G. R. Public health surveillance of infectious diseases: beyond point mutations. *Lancet Microbe* **2**, e53-e54, doi:10.1016/S2666-5247(21)00003-3 (2021).

36 Garcia-Beltran, W. F. *et al.* Multiple SARS-CoV-2 variants escape neutralization by vaccine-induced humoral immunity. *Cell*, doi:10.1016/j.cell.2021.03.013 (2021).

37 Sabino, E. C. *et al.* Resurgence of COVID-19 in Manaus, Brazil, despite high seroprevalence. *Lancet* **397**, 452-455, doi:10.1016/S0140-6736(21)00183-5 (2021).

38 Darby, A. C. & Hiscox, J. A. Covid-19: variants and vaccination. *BMJ* **372**, n771, doi:10.1136/bmj.n771 (2021).

39 Tegally, H. *et al.* Emergence and rapid spread of a new severe acute respiratory syndrome-related coronavirus 2 (SARS-CoV-2) lineage with multiple spike mutations in South Africa. *medRxiv*, 2020.2012.2021.20248640, doi:10.1101/2020.12.21.20248640 (2020).

40 Planas, D. *et al.* Sensitivity of infectious SARS-CoV-2 B.1.1.7 and B.1.351 variants to neutralizing antibodies. *Nat Med*, doi:10.1038/s41591-021-01318-5 (2021).

41 Thomson, E. C. *et al.* The circulating SARS-CoV-2 spike variant N439K maintains fitness while evading antibody-mediated immunity. *bioRxiv*, 2020.2011.2004.355842, doi:10.1101/2020.11.04.355842 (2020).

42 Di Caro A. *et al.* SARS-CoV-2 escape mutants and protective immunity from natural infections or immunizations,. *Clinical Microbiology and Infection,*, doi:https://doi.org/10.1016/j.cmi.2021.03.011. (2021).